

Highly excited hole strength observed in the $^{90}\text{Zr}(\bar{p},d)^{89}\text{Zr}$ reaction

J. Kasagi, G. M. Crawley, E. Kashy, and J. Duffy

National Superconducting Cyclotron Laboratory, Michigan State University, East Lansing, Michigan 48824

S. Gales and E. Gerlic

Institut de Physique Nucléaire, Orsay, France

D. Friesel

Indiana University Cyclotron Laboratory, Bloomington, Indiana 47401

(Received 22 April 1983)

The $^{90}\text{Zr}(\bar{p},d)^{89}\text{Zr}$ reaction has been studied at $E_p=90$ MeV. Using analyzing power measurements, gross structures observed between $E_x\sim 3.4$ and $E_x\sim 7.0$ MeV are deduced to arise mainly from the pickup of $1f_{5/2}$ neutrons. Between 7.0 and 19 MeV, the main strength comes from the $1f_{7/2}$ transfer although $1d_{3/2}$ strength has also been observed between 16.0 and 20.0 MeV of excitation energy.

[NUCLEAR REACTIONS $^{90}\text{Zr}(\bar{p},d)^{89}\text{Zr}$, $E=90$ MeV, measured $\sigma(E,\theta)$, deduced J , π , and S for ^{89}Zr .]

Deeply bound hole states in medium and heavy nuclei observed in one nucleon pickup reactions are characterized by giant resonancelike broad bumps at an excitation energy of several MeV.¹ The single hole strength is considered to be fragmented by the coupling with the collective phonon-particle states² and to a lesser extent with the core polarized states.³ Additional spreading results from the small mixing of these states with many close-lying states. Therefore, the observation of the shape of the deeply bound hole states gives important information about the mechanism of the fragmentation of highly excited states in nuclei.

So far, $1g_{9/2}$ neutron hole states have been extensively studied for the Sn isotopes⁴ and $1g_{9/2}$ proton hole states have been studied for the Pm isotopes.⁵ The results suggested that there exist differences of the spreading mechanism between the neutron and proton hole states.⁵ The $1f_{7/2}$ shell is a more favorable case to study the strength distribution because of its isolation from both valence and inner shells. Recently, the broad bump observed at $E_x\sim 5$ MeV in the $^{90}\text{Zr}(\bar{d},^3\text{He})^{89}\text{Y}$ reaction has been unambiguously assigned to be a $1f_{7/2}$ hole state by analyzing power measurements.⁶ This $1f_{7/2}$ excitation is well separated from the low-lying states and shows a rather symmetric shape with a few peaks around 5 MeV. On the other hand, the $1f_{7/2}$ neutron hole strength, observed in the $^{90}\text{Zr}(^3\text{He},\alpha)^{89}\text{Zr}$ reaction recently reported by Duhamel *et al.*,⁷ was distributed quite differently from the proton hole case. The reported $1f_{7/2}$ neutron hole strength is distributed rather continuously from $E_x\sim 3.5$ to 20 MeV with several peaks around 5 MeV. However, in the latter experiments, unique spin assignments have not been made and therefore the possibility of the existence of $1f_{5/2}$ hole states at $E_x > 3.5$ MeV is not excluded.

We report here the study of the $^{90}\text{Zr}(\bar{p},d)^{89}\text{Zr}$ at 90

MeV, and the results show that the broad structures between $E_x\sim 3.5$ and 7.0 MeV are not $1f_{7/2}$ hole states but mainly $1f_{5/2}$ hole states. As reported in Ref. 8, unambiguous spin assignments were made both by comparing the measured analyzing power in the (\bar{p},d) reaction with the A_y for well known states and also by comparison with DWBA calculations which gave qualitative fits to both $\sigma(\theta)$ and A_y .

The present experiment was performed using a 90 MeV polarized proton beam from the Indiana University Cyclotron. The beam polarization was about $\pm 70\%$ and was measured before and after each run. The spin direction was flipped automatically every minute during data taking. The target used was a self-supporting foil, 10.25 mg/cm² thick enriched to 98% in ^{90}Zr . A ^{58}Ni foil with a thickness of 5 mg/cm² was also bombarded to obtain the empirical angular distribution $[\sigma(\theta)]$ and analyzing powers $[A_y(\theta)]$ for pickup of $1f_{7/2}$, $1f_{5/2}$, $1d_{3/2}$, and $2s_{1/2}$ neutrons.

The outgoing particles were detected in a solid state detector telescope consisting of a Si(Li), ΔE detector and an intrinsic Ge, E detector. Two telescopes were placed at a distance of 50 cm from the target and on both sides of the beam direction. The overall energy resolution was about 120 keV full width at half maximum. Angular distributions were measured from 14° to 45° in 3° steps.

An energy spectrum at 20° is shown in Fig. 1. Because of the angular momentum matching, the ground state ($\frac{9}{2}^+$) and 1.46-MeV state ($\frac{5}{2}^-$) are very prominent among the low-lying states (the contribution from the unresolved 1.52 MeV state reported in Ref. 9 is estimated to be less than 20%). At excitation energies above 3.4 MeV, the gross structures, concluded to be mainly $1f_{7/2}$ hole states,^{4,7,9} are clearly seen above a smooth background which is assumed to connect the minimum yield at

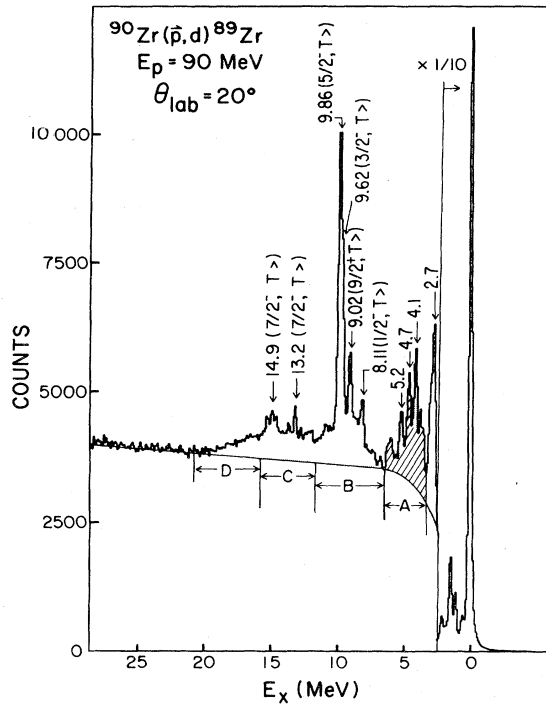


FIG. 1. Energy spectrum of the $^{90}\text{Zr}(p,d)^{89}\text{Zr}$ reaction at $E_p=90$ MeV. The major peaks above 2.5 MeV are labeled by excitation energies in MeV. The shaded and hatched areas in the gross structure above 3.4 MeV show the $(1f_{7/2})^{-1}$ and $(1f_{5/2})^{-1}$ state distributions, respectively. The tail in area D is drawn using the results that half of this area is from $(1d_{3/2})^{-1}$.

$E_x \sim 30, 7,$ and 2.5 MeV. However, the detailed structure observed in the $(^3\text{He},\alpha)$ reaction⁷ is not the same as that seen in the present (p,d) measurement. A clear dip can be seen at about 7 MeV in the present data but no such dip was reported in Ref. 7. The structures observed in the present experiment can be separated into two parts. One of them is the bump with several peaks between 3.4 and 7.0 MeV. Another one is the region lying between 7.0 and 21 MeV. This latter region is rather structureless except for the sharp isobaric analogs of low-lying states of ^{89}Y (labeled $T_>$). They are considered to be analogs of the 5.0 and 6.8 MeV peaks observed in ^{89}Y , because of the similarity in energy spacing and in the shape of the structures observed in the two reactions. The parent states of the 13.2 and 14.9 MeV peaks have been assigned to have $J^\pi = \frac{7}{2}^-$. There was also a broad bump under this peak which was also tentatively assigned a J^π of $\frac{7}{2}^-$.

The spin parity of $\frac{7}{2}^-$ proposed for all these structures in Refs. 7 and 9 was based on the angular distributions and on spectroscopic factor (S -factor) arguments, except for the region near 20 MeV where some $1d$ strength has been reported.⁷ The analyzing power measurements were used to determine the spin of these broad structures. We divided the region between 3.4 and 21 MeV excitation energy into four areas as indicated in the figure. Area A is from 3.4 to 7.0 MeV, B from 7.0 to 11.6 MeV, C from 11.6 to 16 MeV, and D from 16 to 21 MeV. $\sigma(\theta)$ and

$A_y(\theta)$ for each area have been obtained by integrating the yield above background excluding the sharp peaks of the analog states at around 9 MeV. In addition, $\sigma(\theta)$ and $A_y(\theta)$ of the peaks in area A and at 13.2 and 14.9 MeV have also been obtained separately.

The angular distributions of the cross sections for various known states do not show any sensitivity to the orbital angular momentum l of the transferred neutron, except for $l=0$ and 1. However, the $A_y(\theta)$'s are characterized by the number of nodes (N) of the radial wave function and the total angular momentum, j of the transferred nucleon, as reported by Hosono *et al.*¹⁰ For $N=0$ the $A_y(\theta)$ of $j=l+\frac{1}{2}$ has a positive value and a dip around 20° , while that of $j=l-\frac{1}{2}$ has negative values at forward angles and a peak at around 23° . DWBA calculations can explain these characteristic features only qualitatively. Therefore the following arguments for J^π assignments are based on a comparison with the empirical analyzing power.

In Fig. 2 are shown $\sigma(\theta)$ and $A_y(\theta)$ for areas A–D, the 4.1 and 14.9 MeV peaks, and the background under area

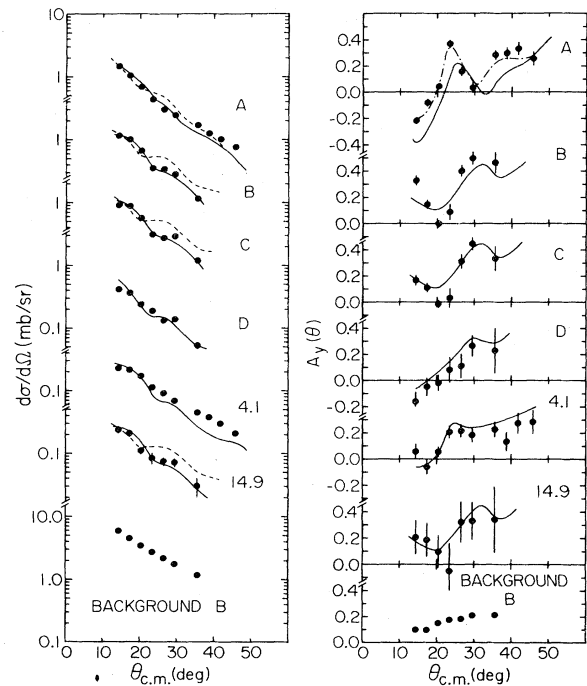


FIG. 2. Angular distributions of cross section (left-hand side) and analyzing power for areas A–D, the 4.1 MeV peak, the 14.9 MeV peak, and the background under area B. Solid lines are empirical angular distributions taken from $^{58}\text{Ni}(\bar{p},d)^{57}\text{Ni}$ (0.76 MeV, $\frac{5}{2}^-$) for area A and ^{57}Ni (2.57 MeV, $\frac{7}{2}^-$) for areas B and C, and the 14.9 MeV peak. The lines drawn for area D and the 4.1 MeV peak are also empirical ones from $^{58}\text{Ni}(\bar{p},d)$ but mixed in such a way that the same yield from $1d_{3/2}$ and $1f_{7/2}$ is assumed at forward angles ($\leq 20^\circ$) for area D and the same yield from $1f_{5/2}$ and $1f_{7/2}$ at forward angles for the 4.1 MeV peak. Dashed lines on the left-hand side of the figure show the results of DWBA calculations for pure transitions. The dashed-dotted line on the right-hand side of the figure is the empirical analyzing power for $\frac{5}{2}^-$ from the ^{89}Zr (1.46 MeV, $\frac{5}{2}^-$) state.

B. The experimental $A_y(\theta)$ clearly show that the main contribution to areas *B* and *C* is the same orbit and is different from that of areas *A* and *D*. The predominant orbital angular momentum transfer for regions *A*–*C* is known to be $l=3$ from Refs. 7 and 9. The main contribution to area *A* is concluded to arise from the $1f_{5/2}$ orbit by comparison with the A_y of the known $\frac{5}{2}^-$ states at 1.46 MeV (^{89}Zr) and at 0.76 MeV (^{57}Ni), as shown in the figure. Among the peaks in this area, the 4.1 and 5.2 MeV peaks have a non-negligible contribution of a $j=l+\frac{1}{2}$ type transition. As the peaks in this region were observed to be populated by an orbital angular momentum transfer of 3, we can conclude that $1f_{7/2}$ strength is present in both peaks. As shown in Fig. 2, the analyzing power of the 4.1 MeV peak is fit qualitatively by an empirical mixture of $1f_{5/2}$ and $1f_{7/2}$ transitions in which the same yield is assumed for the $1f_{5/2}$ and $1f_{7/2}$ transitions at angles forward of 20° .

Areas *B* and *C*, on the other hand, are assigned to correspond mainly to $1f_{7/2}$ neutron transfer since the A_y for these areas matches that for the known $\frac{7}{2}^-$ state in ^{57}Ni at 2.57 MeV, as shown in Fig. 2. In addition, the A_y of the

14.9 MeV peak in ^{89}Zr , which is the analog of the known $\frac{7}{2}^-$ state at 6.8 MeV in ^{89}Y , is also very similar to the A_y of areas of *B* and *C*. This adds further support to the $\frac{7}{2}^-$ assignment.

The A_y of area *D* suggests that it contains components from both $j=l+\frac{1}{2}$ and $l-\frac{1}{2}$. Since the $1f_{5/2}$ strength is already exhausted below $E_x=7.0$ MeV (see Table I), one might expect a contribution from the next lowest $j=l-\frac{1}{2}$ state, viz., $1d_{3/2}$ as was also suggested in Ref. 7. By comparing the empirical A_y 's of the $1d_{3/2}$ from the 8.84 MeV, $\frac{3}{2}^+$ state in ^{57}Ni and $1f_{7/2}$ (area *C*) as shown in the figure, we can conclude that about 50% of the yield in area *D* is from the $1d_{3/2}$ orbit.

In order to obtain the spectroscopic factors DWBA, calculations have been carried out using the code DWUCK4 (Ref. 11) with finite range corrections. The optical potentials used were standard ones obtained from fitting proton and deuteron elastic scattering.^{12,13} The *S* factors for each area are extracted by comparing the DWBA cross sections with the experimental ones at forward angles ($<20^\circ$). Some of the results of the DWBA calculations are shown in Fig. 2 as well as empirical cross sections obtained from

TABLE I. Spectroscopic factors obtained for $^{90}\text{Zr}(p,d)^{89}\text{Zr}$.

nlj	E_x (MeV)	C^2S	Simple shell model prediction	Average excitation energy E_j (MeV)
$1g_{9/2}$	0.	9.6		0.18
	2.75	0.29		
	9.03	0.11		
		10.00 ^a	10	
$2p_{1/2}$	0.60	1.2		1.23
	8.10	0.11		
		1.31	2	
$2p_{3/2}$	1.09	2.1		1.95
	1.87	0.53		
	9.62	0.24		
		2.87	4	
$1f_{5/2}$	1.46	3.5 ^b		3.27 ^c
	2.10	0.66		
	3.0	0.46		
	3.4–7.0	1.7		
	9.86	0.64		
		6.96	6	
$1f_{7/2}$	4.1	0.82		10.3 ^c
	5.2	0.35		
	7.0–11.6	2.8		
	11.6–16.0	2.1		
	16.0–21.0	0.43		
		6.50	8	
$1d_{3/2}$	16.0–21.0	1.2		

^a $1g_{9/2}$ strength normalized to 10.0.

^bContains a small contribution ($<20\%$) from the 1.51 MeV ($\frac{9}{2}^+$) state.

^cThe spectroscopic strength was assumed always to be at the center of the broad regions.

the $^{58}\text{Ni}(p,d)^{57}\text{Ni}$ reaction. The S factors obtained are normalized in such a way that the total S factor of the $1g_{9/2}$ orbit is set equal to the sum-rule limit, and are listed in Table I. These S factors are obtained by using effective binding energies, since the separation energy method gives S factors for isobaric analog states which are too large, as reported in Refs. 7, 9, and 14. The differences in the relative S factors with different optical potentials are found to be less than 20%.

The S factors of the lowest state for each orbit are in reasonable agreement (within 25%) with those reported in Refs. 7, 9, and 14, except for the $\frac{1}{2}^-$ state. The total S factor obtained for $l=1$ transitions is about 70% of the sum rule limit. This might be due to the fact that some of the weak transitions are not clearly observed in this experiment. For the $(1f_{5/2})^{-1}$ states, almost all the strength is exhausted below 7.0 MeV. The previous works reported more $l=3$ strength in the region between 3.5 and 7 MeV than the present result, and suggested a $(1f_{7/2})^{-1}$ assignment. Less $(1f_{7/2})^{-1}$ strength was also reported⁷ above 7 MeV than was found in the present experiment. These discrepancies in the S factors are probably due to the difference between the backgrounds. In the present case, the background is less ambiguous since there exists a minimum in the spectrum at $E_x \sim 7$ MeV and the background can be drawn through this minimum (see Fig. 1). Considering the accuracy of the relative S factors obtained in this experiment, we would conclude that almost all the $(1f_{7/2})^{-1}$ strength has been found between 4 and 20 MeV excitation energy. For the $1d_{3/2}$ transition, only 30% of the sum-rule limit is obtained. This suggests that additional $1d_{3/2}$ strength should be observed in the higher excitation energy region.

Thus, the characteristic feature of the high-lying hole states of ^{89}Zr observed in the (\bar{p},d) reaction can be summarized as follows. The structure between 3.4 and 7.0 MeV, which was previously proposed to be mainly $(1f_{7/2})^{-1}$, has been shown to contain substantial $(1f_{5/2})^{-1}$ strength. The $(1f_{7/2})^{-1}$ strength in this excitation region is found in the 4.1 and 5.2 MeV peaks, which have only 18% of the total observed $(1f_{7/2})^{-1}$ strength. On the other hand, the amount of the $(1f_{5/2})^{-1}$ strength found in this region is about 25% of the total $(1f_{5/2})^{-1}$ strength observed. About half of the total $(1f_{5/2})^{-1}$ strength is concentrated in the 1.46 MeV peak. No $(1f_{5/2})^{-1} T_<$ strength was found above 7 MeV.

Beyond 7 MeV, almost all the $(1f_{7/2})^{-1}$ strength is found in the gross structure which continues up to about 20 MeV. The $T_>$ $(1f_{7/2})^{-1}$ peaks are observed at 13.2 and 14.9 MeV. Therefore, the broad structure of $T_>$ $(1f_{7/2})^{-1}$ states observed in the $(\bar{d}^3\text{He})$ reaction⁶ can be expected to lie between 12 and 19 MeV. However, there is no clear separation between $T_>$ and $T_<$ states. The $T_<$ strength may be distributed very broadly between 7.0 and 15 MeV as well as in the 4.1 and 5.2 MeV peaks.

The present unambiguous spin assignments show that not only the $(1f_{7/2})^{-1}$ states but also the $(1f_{5/2})^{-1}$ states are spread very widely. There is substantial $(1f_{5/2})^{-1}$ strength observed between 3.4 and 7.0 MeV. While the phonon coupling picture gives a good description of the spreading of the $T_<$ states in the tin isotopes,² the fact that the $\frac{3}{2}^-$, $T_>$ state is very sharp and the $(1f_{5/2})^{-1}$, $T_<$ strength is very fragmented implies that the main spreading is probably due to coupling with core polarized states, as discussed by Taketani *et al.*¹⁴ These authors suggest that such core polarization will give rise to a single sharp level at low excitation and several fragmented peaks a few MeV higher in excitation since the core polarized states are expected to be 3 or 4 MeV higher in excitation than the pure $1f_{5/2}$ hole state. The pattern of $\frac{5}{2}^-$ strength observed in the present experiment matches this expectation quite well, thus supporting a core excitation model for the spreading of the $(1f_{5/2})$ hole strength.

In contrast, however, the $(1f_{7/2})$ hole strength does not follow the same pattern. First, the $T_>$ states of $(1f_{7/2})^{-1}$ are widely spread, and second, there is no sharp level with large $(1f_{7/2})^{-1}$ strength comparable to the 1.46 MeV level for the $(1f_{5/2})^{-1}$ case. However, there is some $\frac{7}{2}^-$ strength in the peaks at 4.1 and 5.2 MeV. Thus the core polarization mechanism is probably not the main mechanism for the spreading of the $(f_{7/2}^{-1})$ strength, and coupling with phonon states is probably more important.

In summary, the experiment confirms the $\frac{7}{2}^-$ spin-parity assignment to the broad structure observed between 7 and 11.6 MeV and to the $T_>$ states at 13.2 and 14.9 MeV. However, in contrast to previous work, the present results show significant $(1f_{5/2})^{-1}$ strength between 3.4 and 7 MeV.

This work was supported in part by the National Science Foundation under Grant No. PHY 80 17605, and by Le Centre National de la Recherche Scientifique (France).

¹M. Sakai and K. I. Kubo, Nucl. Phys. **A185**, 217 (1972); S. Gales, *ibid.* **A354**, 193 (1981).

²T. Koeling and F. Iachello, Nucl. Phys. **A295**, 45 (1978); V. G. Soloviev, Ch. Stoyanov, and A. I. Velovin, *ibid.* **A342**, 261 (1980).

³M. Nomura, Prog. Theor. Phys. **55**, 622 (1976).

⁴E. Gerlic *et al.*, Phys. Lett. **57B**, 338 (1975); Phys. Rev. C **21**, 124 (1980); M. Sekiguchi *et al.*, Nucl. Phys. **A278**, 231 (1977); M. Tanaka *et al.*, *ibid.* **78B**, 221 (1978); R. H. Siemssen *et al.*, Phys. Lett. **103B**, 323 (1981).

⁵P. Doll *et al.*, Phys. Lett. **82B**, 357 (1979).

⁶A. Stuirbrink *et al.*, Z. Phys. A **297**, 307 (1980).

⁷G. Duhamel *et al.*, J. Phys. G **7**, 1415 (1981).

⁸G. M. Crawley *et al.*, Phys. Rev. C **23**, 1818 (1981).

⁹S. Gales *et al.*, Nucl. Phys. **A288**, 221 (1977).

¹⁰K. Hosono *et al.*, Nucl. Phys. **A343**, 234 (1980).

¹¹P. D. Kunz (unpublished).

¹²P. Schwandt (private communication).

¹³D. G. Duhamel *et al.*, Nucl. Phys. **A179**, 48 (1971).

¹⁴H. Taketani *et al.*, Nucl. Phys. **A204**, 385 (1973).